

## Phonons in Disordered Si-Ge Alloys

Vipin Srivastava and S. K. Joshi

Physics Department, Roorkee University, Roorkee, India

(Received 30 April 1973)

The coherent-potential approximation for phonons in disordered binary alloys has been used to interpret the observed Raman spectra of the substitutionally disordered Si-Ge alloys. The spectral density function is calculated for the  $\vec{q} = 0$  optical phonons.

### I. INTRODUCTION

Some of the interesting effects in the atomic vibrations of solids arise from the presence of defects in the perfect lattice. In recent years a lot of work has been done on lattice vibrations of disordered alloys. The vibration spectra of a large number of binary and pseudobinary alloys have been studied by means of infrared absorption and Raman scattering.<sup>1</sup> Two distinct types of behavior are found. For some systems only long-wavelength optical-phonon frequencies occur which shift, in most cases, linearly with concentration from the mode frequencies of the lighter component downward to the mode frequencies of the heavier component. In other systems vibration frequencies related to each one of the constituents can be separately found in the middle of the concentration range. The first, or the one-mode-type behavior, is obtained for most of the solid solutions of alkali halides, while the second, or two-mode-type behavior, is found in most solid solutions of zinc-blende-type crystals. Balkanski<sup>2</sup> suggests that the long-range average-crystal-potential variation may have been large enough for the one-mode systems to shift the eigenfrequencies of each constituent towards a unique value, and is not sufficient for the two-mode case. The alkali-halide mixed crystals are strongly ionic in character, and therefore each atom is subjected to electrostatic forces extending much further than the statistical cluster in which it is embedded. These forces, therefore, average for each pair of ions and yield a unique frequency for the mixture. On the contrary, in zinc-blende-type mixed crystals the first-neighbor interaction dominates and is responsible for the splitting of the vibrational spectrum.

A third type of multimode behavior has been reported for the Raman spectra of Ge-Si alloys by Feldman *et al.*<sup>3</sup> over a small composition range (0–33 at. % Si in Ge) and by Renucci *et al.*<sup>4</sup> over the whole composition range. The three peaks are attributed by Renucci *et al.* and Feldman *et al.* to the vibrations of Ge-Ge, Ge-Si, and Si-Si nearest-neighbor pairs. Silicon and germanium form a mixed crystal in all proportions.<sup>5</sup> Because the

silicon mass is much less than that of germanium, one would expect local modes to be associated with the motion of silicon atoms in germanium. Germanium and silicon have a common valency, so that such modes are not expected to be infrared active in first order; however, they should be Raman active. In this paper we have tried to understand the experimental observations for the Ge-Si system by Feldman *et al.*<sup>3</sup> and Renucci *et al.*,<sup>4</sup> theoretically within the framework of the coherent-potential approximation (CPA)<sup>6–8</sup> for the disordered systems.

Section II is essentially a brief review of the work of Taylor,<sup>8</sup> which introduced the CPA within the multiple-scattering formalism for phonons in disordered systems. This helps us in fixing the notation and forms the basis of the results of the calculation. The solution of the spectral function for the particular system Ge-Si and its comparison with the experimental results of Renucci *et al.* and Feldman *et al.* are discussed in Sec. III.

### II. GENERAL FORMULATION

The Hamiltonian for the harmonic lattice containing impurities is

$$H = H_0 + H', \quad (2.1)$$

where

$$H_0 = \sum_{l\kappa} \frac{p^2(l\kappa)}{2M_0} + \frac{1}{2} \sum_{\substack{l, l' \\ \kappa, \kappa'}} \sum_{\alpha, \beta} \Phi_{\alpha\beta}(l\kappa, l'\kappa') u_{\alpha}(l\kappa) u_{\beta}(l'\kappa') \quad (2.2)$$

is the perfect lattice Hamiltonian for a crystal of Ge or Si,  $p(l\kappa)$  is the momentum operator for the atom of mass  $M_0$  in the  $l$ th unit cell with basis index  $\kappa$ , and  $u_{\alpha}(l\kappa)$  is the  $\alpha$ th Cartesian component of the displacement operator for this atom.  $\Phi_{\alpha\beta}(l\kappa, l'\kappa')$  are force constants. If we confine ourselves to the mass disorder only we have

$$H' = \sum_{l\kappa} \frac{p^2(l\kappa)}{2} \left( \frac{1}{M(l\kappa)} - \frac{1}{M_0} \right). \quad (2.3)$$

Such an assumption makes the disorder cell localized. Contributions to  $H'$  come from impurity

sites only. An examination of the optical modes of germanium<sup>9</sup> and silicon<sup>10</sup> in directions [100] and [110], obtained through neutron-scattering measurements by Ghose *et al.*<sup>9</sup> and Dolling,<sup>10</sup> respectively, shows that the optical phonons scale by numbers which lie between 0.58 and 0.61. This is reasonably close to  $(M_{Si}/M_{Ge})^{1/2} = 0.62$ . This encouraged us to take into account only the mass change in the present calculation.

The displacement-displacement double-time thermal Green's functions<sup>11</sup> are defined as

$$\begin{aligned} G_{\alpha\beta}^{\text{ret}}(l\kappa, l'\kappa'; t-t') &= 2\pi \langle \langle u_\alpha(l\kappa, t); u_\beta(l'\kappa', t') \rangle \rangle_{\text{ret}} \\ &= -2\pi i \langle [u_\alpha(l\kappa, t), u_\beta(l'\kappa', t')] \rangle_T \theta(t-t'), \quad (2.4a) \end{aligned}$$

$$\begin{aligned} G_{\alpha\beta}^{\text{adv}}(l\kappa, l'\kappa'; t-t') &= 2\pi \langle \langle u_\alpha(l\kappa, t); u_\beta(l'\kappa', t) \rangle \rangle_{\text{adv}} \\ &= 2\pi i \langle [u_\alpha(l\kappa, t), u_\beta(l'\kappa', t')] \rangle_T \theta(t'-t), \quad (2.4b) \end{aligned}$$

$$\theta(t) = 1, \quad t > 0$$

$$= 0, \quad t < 0.$$

$\alpha, \beta$  denote the Cartesian components and  $\langle \rangle_T$  denotes the thermal average. The average over different configurations is denoted simply by  $\langle \rangle$ . The Fourier time transform of  $G$  is given by

$$G_{\alpha\beta}(l\kappa, l'\kappa'; \omega \pm i\delta) = \frac{1}{2\pi} \int_{-\infty}^{\infty} G_{\alpha\beta}^{\text{ret, adv}}(l\kappa, l'\kappa'; t) \times e^{i(\omega \pm i\delta)t} dt. \quad (2.5)$$

We shall suppress the infinitesimal quantity  $\delta$  and understand that for the retarded and advanced cases  $\omega$  approaches the real axis from the upper and lower half-planes, respectively. For a harmonic lattice, both Green's functions of (2.4) for a system described by Eqs. (2.1)–(2.3) satisfy identical second-order differential equations of motion which, when transformed according to (2.5), give the following equation for  $G$ :

$$\begin{aligned} -M_0\omega^2 G_{\alpha\beta}(l\kappa, l'\kappa'; \omega) &+ \sum_{\substack{l''\kappa'' \\ \kappa''\gamma}} \Phi_{\alpha\gamma}(l\kappa, l''\kappa'') G_{\gamma\beta}(l''\kappa'', l'\kappa'; \omega) \\ &= -\delta_{\alpha\beta} \delta(l\kappa, l'\kappa') \\ &+ \sum_{\substack{l''\kappa'' \\ \kappa''\gamma}} C_{\alpha\gamma}(l\kappa, l''\kappa'') G_{\gamma\beta}(l''\kappa'', l'\kappa'; \omega), \quad (2.6) \end{aligned}$$

$$C_{\alpha\beta}(l\kappa, l'\kappa'; \omega) = [M_0 - M(l\kappa)] \omega^2 \delta_{\alpha\beta} \delta(l\kappa, l'\kappa'). \quad (2.7)$$

For a defect atom at  $l_i\kappa_i$ , it is convenient to describe the change in mass,

$$M_0 - M(l_i\kappa_i) = M_0 \epsilon^{(l_i\kappa_i)}, \quad (2.8)$$

by the matrix

$$C_{\alpha\beta}^{(l_i\kappa_i)}(l\kappa, l'\kappa'; \omega) = M_0 \epsilon^{(l_i\kappa_i)} \omega^2 \delta_{\alpha\beta} \delta(l\kappa, l'\kappa') \delta(l\kappa, l_i\kappa_i). \quad (2.9)$$

$\epsilon^{(l_i\kappa_i)}$  therefore gives the fractional mass change at  $(l_i\kappa_i)$  occupied by an atom of type  $p$ . If the Green's function for the perfect lattice [i. e.,  $\underline{C} = 0$  in Eq. (2.6)], denoted by  $\underline{P}$ , is known, then one obtains for  $\underline{G}$

$$\begin{aligned} G_{\alpha\beta}(l\kappa, l'\kappa'; \omega) &= P_{\alpha\beta}(l\kappa, l'\kappa'; \omega) \\ &+ M_0 \epsilon \omega^2 \sum_{\substack{s, \gamma \\ \kappa_s}} P_{\alpha\gamma}(l\kappa, s\kappa_s; \omega) G_{\gamma\beta}(s\kappa_s, l'\kappa'; \omega). \quad (2.10) \end{aligned}$$

( $s\kappa_s$ ) denotes the impurity site. Now

$$\begin{aligned} P_{\alpha\beta}(l\kappa, l'\kappa'; \omega) &= \frac{1}{NM_0} \sum_{\vec{q}, j} \frac{\sigma_\alpha^{j*}(\vec{q}) \sigma_\beta^j(\vec{q}) e^{-i\vec{q} \cdot (\vec{R}_{l\kappa} - \vec{R}_{l'\kappa'})}}{\omega^2 - \omega_j^2(\vec{q})}; \quad (2.11) \end{aligned}$$

$N$  is the number of unit cells and  $j$  specifies the  $3s$  branches, where  $s$  is the number of atoms per unit cell.  $\omega_j(\vec{q})$  are the eigenvalues and  $\sigma_\alpha^j(\vec{q})$  are the eigenvectors of the dynamical matrix for a perfect crystal. Equation (2.10) for the Green's function of the imperfect crystal  $\underline{G}$  can be rewritten in the form

$$\begin{aligned} \underline{G}(l\kappa, l'\kappa'; \omega) &= \underline{P}(l\kappa, l'\kappa'; \omega) \\ &+ \sum_{\substack{l_1\kappa_1, l_2\kappa_2 \\ \kappa_1, \kappa_2}} \underline{P}(l\kappa, l_1\kappa_1; \omega) \underline{C}(l_1\kappa_1, l_2\kappa_2; \omega) \underline{G}(l_2\kappa_2, l'\kappa'; \omega), \quad (2.12) \end{aligned}$$

where the defect matrix is given by

$$\underline{C}(l\kappa, l'\kappa'; \omega) = \sum_{l_i\kappa_i} \underline{C}^{(l_i\kappa_i)}(l\kappa, l'\kappa'; \omega). \quad (2.13)$$

Equation (2.12) is the usual Dyson equation with  $\underline{C}$  as perturbation. If we introduce the  $\underline{T}$  matrix,

$$\underline{T}(l_1\kappa_1, l_2\kappa_2; \omega) = \frac{\underline{C}(l_1\kappa_1, l_2\kappa_2; \omega)}{1 - \underline{C}(l_1\kappa_1, l_2\kappa_2; \omega) \underline{P}(l_1\kappa_1, l_2\kappa_2; \omega)}, \quad (2.14)$$

we can write

$$\begin{aligned} \underline{G}(l\kappa, l'\kappa'; \omega) &= \underline{P}(l\kappa, l'\kappa'; \omega) \\ &+ \sum_{\substack{l_1\kappa_1, l_2\kappa_2 \\ \kappa_1, \kappa_2}} \underline{P}(l\kappa, l_1\kappa_1; \omega) \underline{T}(l_1\kappa_1, l_2\kappa_2; \omega) \\ &\quad \times \underline{P}(l_2\kappa_2, l'\kappa'; \omega). \quad (2.15) \end{aligned}$$

Averaging (2.15) over all configurations, we have

$$\begin{aligned} \langle \underline{G}(l\kappa, l'\kappa'; \omega) \rangle &= \underline{P}(l\kappa, l'\kappa'; \omega) \\ &+ \sum_{\substack{l_1\kappa_1, l_2\kappa_2 \\ \kappa_1, \kappa_2}} \underline{P}(l\kappa, l_1\kappa_1; \omega) \langle \underline{T}(l_1\kappa_1, l_2\kappa_2; \omega) \rangle \\ &\quad \times \underline{P}(l_2\kappa_2, l'\kappa'; \omega). \quad (2.16) \end{aligned}$$

On iterating Eq. (2.12) and averaging, we have the result in terms of the self-energy  $\underline{\Sigma}$ :

$$\begin{aligned} \langle \underline{G}(l\kappa, l'\kappa'; \omega) \rangle &= \underline{P}(l\kappa, l'\kappa'; \omega) \\ &+ \sum_{\substack{l_1\kappa_1, l_2\kappa_2 \\ \kappa_1, \kappa_2}} \underline{P}(l\kappa, l_1\kappa_1; \omega) \underline{\Sigma}(l_1\kappa_1, l_2\kappa_2; \omega) \\ &\quad \times \langle \underline{G}(l_2\kappa_2, l'\kappa'; \omega) \rangle. \quad (2.17) \end{aligned}$$

Now we make an approximation  $\underline{E}$  for the actual self-energy  $\underline{\Sigma}$ . A new Green's function is defined in terms of  $\underline{E}$  as

$$\begin{aligned} \underline{G}^0(l\kappa, l'\kappa'; \omega) = & \underline{P}(l\kappa, l'\kappa'; \omega) \\ & + \sum_{\substack{l_1, l_2 \\ \kappa_1, \kappa_2}} \underline{P}(l\kappa, l_1\kappa_1; \omega) \underline{E}(l_1\kappa_1, l_2\kappa_2; \omega) \\ & \times \underline{G}^0(l_2\kappa_2, l'\kappa'; \omega). \end{aligned} \quad (2.18)$$

Then writing Eq. (2.12) in terms of  $\underline{G}^0$  rather than  $\underline{P}$ , we obtain

$$\begin{aligned} \underline{G}(l\kappa, l'\kappa'; \omega) = & \underline{G}^0(l\kappa, l'\kappa'; \omega) \\ & + \sum_{\substack{l_1, l_2 \\ \kappa_1, \kappa_2}} \underline{G}^0(l\kappa, l_1\kappa_1; \omega) \underline{V}^{(l_2\kappa_2)}(l_1\kappa_1, l_2\kappa_2; \omega) \\ & \times \underline{G}(l_2\kappa_2, l'\kappa'; \omega), \end{aligned} \quad (2.19)$$

with

$$\begin{aligned} \underline{V}^{(l_2\kappa_2)}(l_1\kappa_1, l_2\kappa_2; \omega) = & -\underline{E}(l_1\kappa_1, l_2\kappa_2; \omega) \\ & \text{for a host atom at } l_2\kappa_2 \\ = & -\underline{E}(l_1\kappa_1, l_2\kappa_2; \omega) \quad (2.20a) \\ & + M_0 c \omega^2 \delta(l_1\kappa_1, l_2\kappa_2) \underline{I} \\ & \text{for a defect atom at } l_2\kappa_2. \end{aligned} \quad (2.20b)$$

In the single-site CPA we choose our system such that besides the site, say,  $(l\kappa)$  (which has the liberty of being occupied by the host atom or the defect atom), all the rest of the sites are configurationally averaged. If we identify  $\underline{E}$  with the exact  $\underline{\Sigma}$ , then  $\underline{G}^0$  becomes equal to the exact  $\langle \underline{G} \rangle$  and the self-consistency condition for determining  $\underline{E}$  is<sup>8</sup>

$$\sum_p c^p \underline{T}^p(\vec{q}, \omega) = 0. \quad (2.21)$$

$c^p$  is the concentration of the  $p$ -type atoms in the lattice and hence is proportional to the probability of the occurrence of a  $p$ -type atom at a site.  $\underline{T}$  is calculated in terms of the modified Green's function  $\underline{G}^0$ . Equation (2.21) is

$$(1-c)\underline{T}^h + c\underline{T}^d = 0,$$

with

$$\underline{T}^p = \frac{\underline{V}^p}{1 - \underline{G}^0 \underline{V}^p},$$

where  $h$  and  $d$  stand for host and defect, respectively. The explicit form of  $\underline{V}^p$  is given in Eq. (2.20) and on simplification we get

$$\begin{aligned} \underline{E}(\vec{q}, \omega) \left( \underline{I} + \frac{1}{N} \sum_{\vec{q}} \underline{G}^0(\vec{q}, \omega) \underline{E}(\vec{q}, \omega) \right)^{-1} \\ \times \left( \underline{I} - (1-c)M_0 c \omega^2 \underline{G}^0(\omega) \right. \\ \left. + \frac{1}{N} \sum_{\vec{q}} \underline{G}^0(\vec{q}, \omega) \underline{E}(\vec{q}, \omega) \right) = M_0 c \omega^2 \underline{I}, \end{aligned} \quad (2.22)$$

where

$$\underline{G}^0(\omega) = \underline{G}^0(l\kappa, l\kappa; \omega) = \frac{1}{N} \sum_{\vec{q}} \underline{G}^0(\vec{q}, \omega). \quad (2.23)$$

Thus  $\underline{E}(\vec{q}, \omega)$  is independent of  $\vec{q}$ , so that

$$\frac{1}{N} \sum_{\vec{q}} \underline{G}^0(\vec{q}, \omega) \underline{E}(\vec{q}, \omega) = \underline{G}^0(\omega) \underline{E}(\omega),$$

and on further simplification Eq. (2.22) becomes

$$\underline{E}(\omega) - M_0 c \omega^2 \underline{I} - \underline{E}(\omega) [M_0 c \omega^2 \underline{I} - \underline{E}(\omega)] \underline{G}^0(\omega) = 0. \quad (2.24)$$

We write

$$\underline{E}(\omega) = M_0 \tilde{\epsilon}(\omega) \omega^2 \underline{I}, \quad (2.25)$$

convert (2.18) into  $\vec{q}$  representation, and change the unperturbed Green's function (2.11) from normal coordinate representation to  $qj$  representation. This enables us to write

$$\underline{G}^0(\omega) = \frac{1}{M_0} \int \frac{\rho(\omega')}{\omega'^2 [1 - \tilde{\epsilon}(\omega)] - \omega'^2} d\omega', \quad (2.26)$$

with

$$\rho(\omega') = \frac{1}{N} \sum_{\vec{q}, j} \delta\{\omega_j(\vec{q}) - \omega'\}, \quad (2.27)$$

which is the phonon density of states of the unperturbed host crystal. Writing (2.26) as

$$\underline{G}^0(\omega) = (1/M_0) \mathcal{G}^0(\omega)$$

and using (2.25), we write (2.24), finally, in the form

$$\tilde{\epsilon}(\omega) - c \epsilon = \tilde{\epsilon}(\omega) [\epsilon - \tilde{\epsilon}(\omega)] \omega^2 \mathcal{G}^0(\omega), \quad (2.28)$$

where

$$\mathcal{G}^0(\omega) = \int \frac{\rho(\omega')}{\omega'^2 [1 - \tilde{\epsilon}(\omega)] - \omega'^2} d\omega'. \quad (2.29)$$

The averaged Green's function  $\langle G(\vec{q}, \omega) \rangle$  is specified by the spectral density

$$\alpha(\vec{q}j, \omega) = -\pi^{-1} \text{Im} \langle G(\vec{q}j, \omega) \rangle. \quad (2.30)$$

We can cast the spectral density function into a form which is convenient for calculation. From Eqs. (2.26) and (2.27) we have

$$\underline{G}^0(\omega) = \frac{1}{NM_0} \sum_{\vec{q}} \int \frac{\delta\{\omega_j(\vec{q}) - \omega'\}}{\omega'^2 [1 - \tilde{\epsilon}(\omega)] - \omega'^2} d\omega'. \quad (2.31)$$

$\underline{G}^0(\omega)$  may be written in terms of the modes specified by  $\vec{q}, j$  as

$$\underline{G}^0(\omega) = \frac{1}{N} \sum_{\vec{q}, j} \underline{G}^0(\vec{q}j, \omega), \quad (2.32)$$

where

$$\begin{aligned} \underline{G}^0(\vec{q}j, \omega) = & (1/M_0) \\ & \times \{ [\omega^2 [1 - \text{Re} \tilde{\epsilon}(\omega)] - \omega_j^2(\vec{q})] - i\omega^2 \text{Im} \tilde{\epsilon}(\omega) \}^{-1}. \end{aligned} \quad (2.33)$$

In the CPA

$$\langle G(\vec{q}j, \omega) \rangle = \underline{G}^0(\vec{q}j, \omega).$$

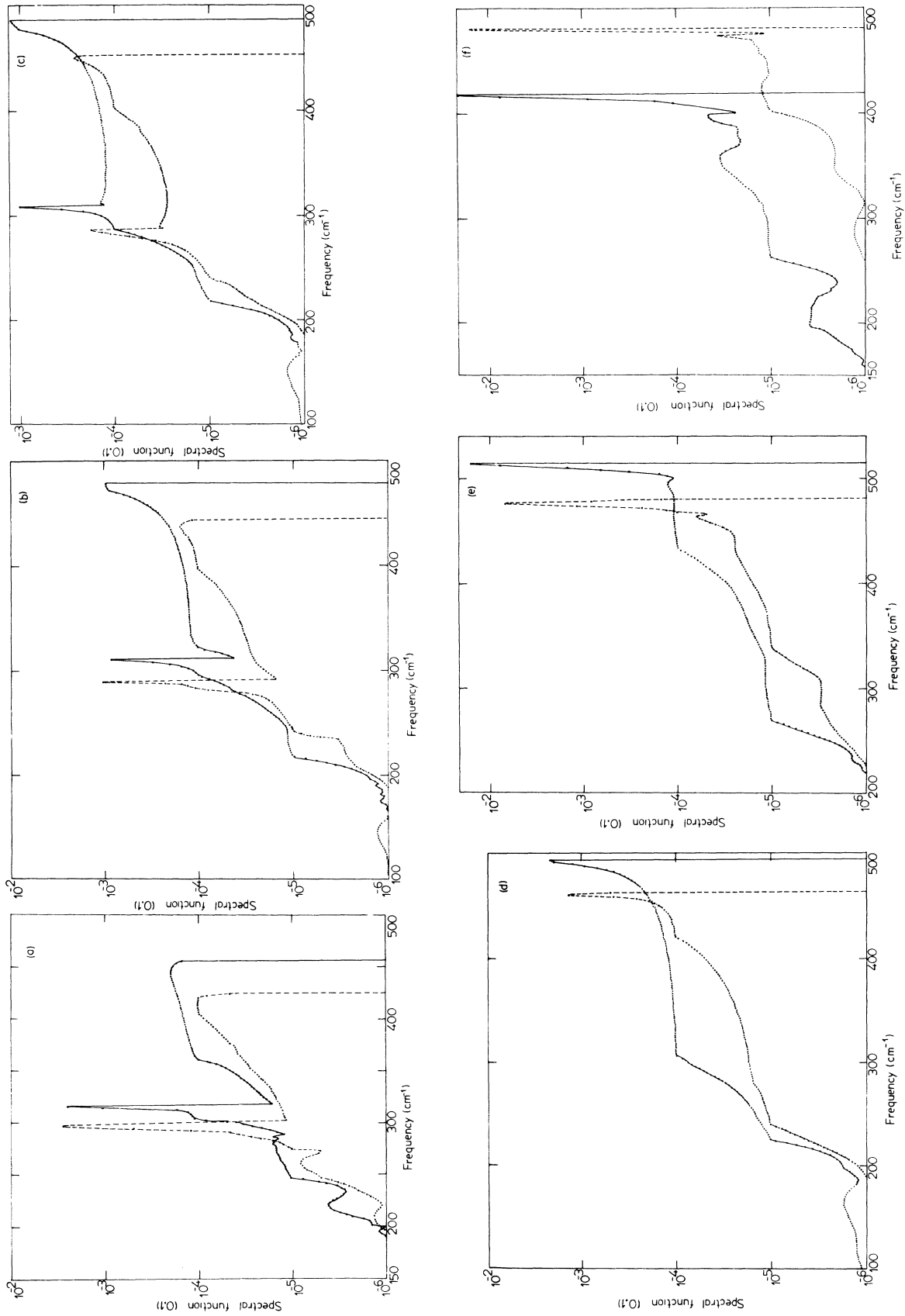


FIG. 1. Plot of spectral density function vs frequency for (a) 10 at. % Si, (b) 25 at. % Si, (c) 35 at. % Si, (d) 54 at. % Si, (e) 85 at. % Si, and (f) 95 at. % Si (solid line denotes Si as host and broken line denotes Ge as host lattice).

Separating the real and imaginary parts in (2.33), we get for the imaginary part

$$\text{Im}\langle G(\vec{q}j, \omega) \rangle = \frac{1}{M_0} \times \frac{\omega^2 \text{Im}\bar{\epsilon}(\omega)}{\{\omega^2[1 - \text{Re}\bar{\epsilon}(\omega)] - \omega_j^2(\vec{q})\}^2 + \{\omega^2 \text{Im}\bar{\epsilon}(\omega)\}^2} \quad (2.34)$$

This gives the spectral density, which can be evaluated by calculating the self-energy from the self-consistent equations (2.28) and (2.29). The function  $\rho(\omega')$  has been taken from Dolling and Cowley's calculations<sup>12</sup> based on their neutron spectroscopic measurements for Ge and Si. The density of states is taken as a histogram of very closely spaced points and integration of (2.29) is done using Simpson's rule, with an initial appropriate choice of  $\bar{\epsilon}(\omega)$ . At low frequencies one can expect from (2.28) that  $\text{Re}\bar{\epsilon}(\omega) \approx c\epsilon$  ( $\epsilon = 0.613$  for a Si-Ge alloy, with Ge taken as host). So the starting point is taken at low frequency, and as an appropriate choice of  $\bar{\epsilon}(\omega)$  we take  $c\epsilon$  as its real part and give some sufficiently large value for its imaginary part in order that the final result may converge at a complex root. Equation (2.28) is then solved. The value of  $\bar{\epsilon}(\omega)$  thus found is again fed back into (2.29) according to the scheme specified in the Newton-Raphson method applied to a function of a complex variable. Equations (2.28) and (2.29) are thus solved by this iterative procedure. Thereafter we calculate the spectral density function from (2.34) for  $\vec{q}=0$  optical modes of Si-Ge alloys. We then proceed to higher frequencies in small steps of  $\omega$ , using the previous value of  $\bar{\epsilon}(\omega)$  as the starting point at each stage. The most difficult region for solving (2.28) and (2.29) is that in which a gap develops in  $\bar{\epsilon}(\omega)$ , where  $\bar{\epsilon}(\omega)$  varies rapidly with  $\omega$  and even diverges at higher concentrations. In the process of the calculation, as soon as we reach the gap from lower frequencies, we switch over to the top of the band and then come down in small steps of  $\omega$  till we again reach the gap. This way we avoid the region of the gap where the calculation diverges. Around the gap the  $\text{Re}\bar{\epsilon}(\omega)$  varies tremendously in a very small frequency range. In this range the frequency grid is made very very narrow. The results are discussed in Sec. III.

### III. RESULTS AND DISCUSSION

The peaks of the spectral density function for optical modes at  $\vec{q}=0$  in this calculation give information about the zone-center optical vibrations of alloys of Ge and Si, either of the two taken as the host crystal. For low concentrations of Ge in Si, one of these may be identified as being due to the heavy defect resonance and the other is near the optical frequency of Si. In our calculations we find that the spectral function shows two distinct

peaks. In the impurity band region the spectral function is not sharply peaked, and peaks are too broad to be called peaks. As the defect concentration increases, the weaker peak becomes merely a shoulder on the larger peak (cf. Fig. 1). At any concentration, the more prominent peak is attributed to the majority atoms. With germanium taken as host lattice, when silicon is added in small quantity it gives rise to a very weak and broad resonance, but this resonance gains prominence as more and more silicon is added. At the middle of the concentration range, the two peaks are of comparable prominence, and as more Si is added the lower peak gradually loses prominence while the upper peak becomes narrower. Eventually the lower peak appears only as a shoulder to the upper peak, which approaches optical frequency for pure silicon. When Si is taken as host and Ge is added to it, the similar structure of peaks is seen throughout the composition range with a shift in the frequency scale. The peaks at all compositions are shifted to slightly higher frequencies and the amount of shift remains almost constant. This shift may be attributed to the changes in force constants during the alloying process. In our calculations we have not considered the changes in force constants that accompany the alloying process. When Ge is taken as host we have assumed the

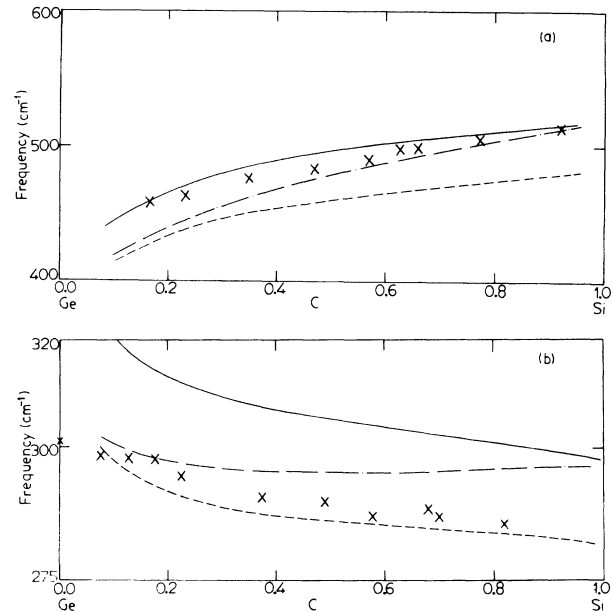


FIG. 2. Plot of (a) frequency of the upper peak vs Si concentration and (b) frequency of the lower peak vs Si concentration [solid line denotes Si as host, broken line denotes Ge as host, dot-dash line denotes the average with concentrations as weighting factors, and  $\times$ 's denote the experimental measurements by Renucci *et al.* (Ref. 4)].

force constants to be the same for the alloy as for pure Ge. Similarly, with Si we take the alloy force constants to be identical to those of Si. In order to take into account in an approximate manner the force-constant changes due to alloying, we have done all calculations by first taking Ge as a host, then taking Si as a host lattice, and finally taking the average of the two values after weighting them with the concentration of that constituent which is regarded as host in the corresponding calculation. This appears to be reasonable and has the appearances of a virtual crystal approximation for the force constants. We shall mention only these weighted averages of force constants in our further discussion.

The variation of the frequencies assigned to the peak in the spectral function with the variation of the Si concentration is shown in Fig. 2. The lower peak shows only slight variation with composition. The frequency decreases as the silicon content increases. The maximum variation, when Ge was host, was observed to be  $16\text{ cm}^{-1}$ ; when Si was host it was  $20\text{ cm}^{-1}$ . These variations for the frequency of the upper peak were  $76$  and  $74\text{ cm}^{-1}$ , respectively, in the two cases. The slight decrease in the lower frequency with increasing Si content obtained in our calculations does not agree with the experimental results of Chang, Lacina, and Pershan,<sup>13</sup> but is in agreement with the observations of Feldman *et al.*<sup>3</sup> and Renucci *et al.*<sup>4</sup> At 33 at. % Si the calculated downward shift is about 7% of the Ge optical-mode frequency. Xinh<sup>14</sup> has treated Raman scattering of light by crystals of the diamond structure containing substitutional random-mass defects and no force-constant changes. He obtained theoretical expressions for the Raman scattering using a self-energy calculated to lowest order in the concentration of the minority atoms.<sup>15</sup> His results should be valid, therefore, only for small concentrations. These results, when applied to Si in Ge, show that the Raman-active localized-mode frequency for small finite concentrations is slightly higher than the localized-mode frequency for a single mass defect. The theory also predicts that the peak in the Raman spectra of the disordered crystal which corresponds to the optical mode ( $\vec{q} \approx 0$ ) of the perfect Ge crystal should shift to lower frequencies with increasing Si concentration.

As may be seen from Fig. 2, the upper peaks obtained by Renucci *et al.*, which they assign to be Si-Si nearest-neighbor vibrations, are very close to the upper peaks obtained by us taking Si as host, i. e., assuming atoms to be joined by the Si-Si force constant in the alloy. Similarly, the so-called Ge-Ge peaks of Renucci *et al.* fall very close to our peaks obtained by taking Ge as host where Ge-Ge force constants are assumed to prevail in the whole lattice. The upper peaks obtained by taking weighted averages fall close to the upper peaks obtained with Ge base at small concentrations of Si and move close to the upper peaks obtained with Si base as the Si concentration increases. Similar behavior is seen with the lower peaks also. The averaged behavior in both cases is pretty well in agreement with the behavior obtained experimentally by Renucci *et al.* A better agreement of the calculation with the experimental measurements could be obtained if, along with the mass change, force-constant changes are also taken into account.

It is also worth noticing that many of the peaks have characteristic asymmetry; they are sharp on the high-frequency side and broader at lower frequencies. This is consistent with the CPA theory. The CPA gives the sharp edges of the bands of the density of states, consequently lopsided spectral functions for the phonons belonging to the  $\vec{q}$  values at these edges.<sup>7</sup> We are concerned with the top of the optical band; hence the peaks obtained by us are sharp at the high-frequency side.

Feldman *et al.* and Renucci *et al.* have assigned the three peaks to the vibrations of the pairs Ge-Ge, Ge-Si, and Si-Si. Our calculations are based on the CPA, which is only the single-site approximation treated self-consistently. This approximation by its nature smooths out the structures due to pairs or clusters, so we do not assign the peaks in our results to the pair vibrations. The nature of our upper and lower peaks is in correspondence with the upper and lower peaks obtained by Feldman *et al.* and Renucci *et al.*

#### ACKNOWLEDGMENTS

One of the authors (S. K. J.) wishes to acknowledge financial support from the Council of Scientific and Industrial Research (India) and the National Bureau of Standards (U. S. A.).

<sup>1</sup>For reference see G. Lucovsky, M. H. Brodsky, and E. Burstein, *Phys. Rev. B* **2**, 3295 (1970).

<sup>2</sup>M. Balkanski, R. Besserman, and J. M. Besson, *Solid State Commun.* **4**, 201 (1961).

<sup>3</sup>D. W. Feldman, M. Ashkin, and James H. Parker, Jr., *Phys. Rev. Lett.* **17**, 1209 (1966).

<sup>4</sup>M. A. Renucci, J. B. Renucci, and M. Cardona, in *Proceedings of the Second International Conference on Light Scattering in Solids*, edited by M. Balkanski (Flammarion, Paris, 1971), p.

326.

<sup>5</sup>J. P. Dismukes, L. Ekstrom, and R. J. Paff, *J. Phys. Chem.* **68**, 3021 (1964).

<sup>6</sup>P. Soven, *Phys. Rev.* **156**, 809 (1967).

<sup>7</sup>B. Velický, S. Kirkpatrick, and H. Ehrenreich, *Phys. Rev.* **175**, 747 (1968).

<sup>8</sup>D. W. Taylor, *Phys. Rev.* **156**, 1017 (1967).

<sup>9</sup>A. Ghose, H. Palevsky, D. J. Hughes, I. Pelah, and C. M. Eisenhauer, *Phys. Rev.* **113**, 49 (1959).

- <sup>10</sup>G. Dolling, *Inelastic Scattering of Neutrons in Solids and Liquids* (International Atomic Energy Agency, Vienna, 1963), Vol. II, p. 37.
- <sup>11</sup>D. N. Zubarev, *Usp. Fiz. Nauk* **71**, 71 (1960) [Sov. Phys.-Usp. **3**, 320 (1960)].
- <sup>12</sup>G. Dolling and R. A. Cowley, *Proc. Phys. Soc. Lond.* **88**, 463 (1966).
- <sup>13</sup>R. K. Chang, Brad Lacina, and P. S. Pershan, *Phys. Rev. Lett.* **17**, 755 (1966).
- <sup>14</sup>N. X. Xinh, Westinghouse Research Laboratories Scientific Paper No. 65-9F5-442-P8, 1965 (unpublished).
- <sup>15</sup>A. A. Maradudin, *Astrophysics and the Many Body Problem* (Benjamin, New York, 1963).